



Fermi National Accelerator Laboratory

FERMILAB-Conf-95/178-E

D0 and CDF

W/Z + Jets Production at the Tevatron

J. Yu

For the D0 and CDF Collaborations

*Fermi National Accelerator Laboratory
P.O. Box 500, Batavia, Illinois 60510*

*University of Rochester
Rochester, New York 14627*

July 1995

Published Proceedings for the *10th Topical Workshop on Proton-Antiproton Collider Physics*,
Fermilab, Batavia, Illinois, May 9-13, 1995

Disclaimer

This report was prepared as an account of work sponsored by an agency of the United States Government. Neither the United States Government nor any agency thereof, nor any of their employees, makes any warranty, expressed or implied, or assumes any legal liability or responsibility for the accuracy, completeness, or usefulness of any information, apparatus, product, or process disclosed, or represents that its use would not infringe privately owned rights. Reference herein to any specific commercial product, process, or service by trade name, trademark, manufacturer, or otherwise, does not necessarily constitute or imply its endorsement, recommendation, or favoring by the United States Government or any agency thereof. The views and opinions of authors expressed herein do not necessarily state or reflect those of the United States Government or any agency thereof.

W/Z + Jets Production at the Tevatron ¹

Jaehoon Yu ²

(for the DØ and CDF Collaborations)

*Department of Physics & Astronomy
University of Rochester
Rochester, New York 14627, U.S.A.*

Both the DØ and CDF experiments at Fermilab Tevatron collider at $\sqrt{s} = 1.8$ TeV have accumulated over 50pb^{-1} of data. Each experiment collected more than 50,000 $W \rightarrow l + \nu$ and 5000 $Z \rightarrow l + \bar{l}$ candidates for each lepton species (e and μ). Using this large data sample of W and Z candidates, the two experiments are actively testing perturbative QCD predictions. Among the studies that are in progress, preliminary results of W/Z+jets characteristics, multiplicity distributions of associated jets, and a study on the determination of the strong coupling constant using the ratio of the $W+1$ jet to $W+0$ jet cross sections are presented.

I. INTRODUCTION

Perturbative Quantum Chromodynamics (pQCD) has been successful in describing experimental data involving jets in the final states. However, testing QCD predictions using the jet final states suffers from inherent experimental and theoretical uncertainties. This is due to the uncertainties involved in defining jets consistently in experiment and in theory, despite the local parton-hadron duality theorem (1). The jet final states also allow a wide range of choices of momentum transfer scale (Q^2) which makes the theoretical predictions unreliable in some regions of Q^2 .

Final states with W or Z bosons have many advantages in testing QCD predictions. Experimentally, these events are easy to identify with relatively small background contamination. Theoretically, the predictions can be made with relatively less uncertainty due to the high momentum transfer scale ($Q^2 \sim M_W^2$ or M_Z^2) of the processes. Note that the W and Z are colorless, giving cleaner final states than jets. (In some ways the inverse of $e^+e^- \rightarrow$ jets with colored particles emerging from the colorless initial states.) These processes are also very important in understanding the background to top production, such as the $t\bar{t} \rightarrow l + jets$ channel.

In addition, the production cross sections of the W and Z bosons are relatively larger at the Tevatron energy ($\sqrt{s} = 1.8$ TeV) compared to other accelerators. More than 50,000 $W \rightarrow l + \nu$ and 5000 $Z \rightarrow l + \bar{l}$ events for each lepton species (e or μ) were accumulated and a factor of two increase in statistics is expected by the end of the current run. The resulting large samples of W and Z boson events will provide a very good opportunity for testing QCD predictions.

¹Talk given at 10th Topical Workshop on Proton Antiproton Collider Physics, May 19 - 13, 1995, Fermilab, Batavia, Illinois

²Author supported by the National Science Foundation of the US government.

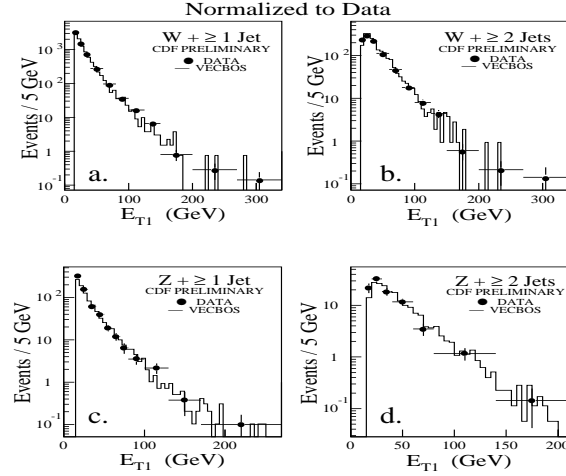


FIG. 1. Leading jet E_T spectra for: (a) $W + \geq 1$ jet, (b) $W + \geq 2$ jet (c) $Z + \geq 1$ jet, and (d) $Z + \geq 2$ jet events. Solid circles represent the data and the histograms illustrate LO predictions.

Some preliminary results on the kinematic characteristics of jets associated with W and Z bosons from the CDF experiment based on 72.9 pb^{-1} of data are presented. Raw jet multiplicity distributions in association with W and Z bosons from the CDF experiment and from the $D\bar{O}$ experiment based on 12.5 pb^{-1} of data are presented followed by a study of the strong coupling constant, α_s , using the ratio of the cross sections of the $W + 1$ jet to $W + 0$ jet processes.

II. W/Z+JETS CHARACTERISTICS

A. Leading jet E_T spectra

The leading jet E_T spectrum of QCD multijet processes generally falls as $E_T^{-(5\sim 6)}$ due to the massless nature of the partons in the final state and the shapes of the parton distribution functions (pdf). In contrast, the spectra in $W/Z + N$ jet events fall less steeply ($E_T^{-(1.5\sim 2)}$). Figure 1 shows the comparison of the spectra for: a) $W + \geq 1$ jet, b) $W + \geq 2$ jet, c) $Z + \geq 1$ jet, and d) $Z + \geq 2$ jet events compared to a leading order (LO) prediction (2) incorporated with the CDF detector simulation (3). The theoretical predictions are normalized to the data so that the shapes can be compared easily. The shape of the observed E_T spectra are well described by the theoretical prediction within the given statistics including the effect of the minimum jet E_T threshold (E_T^{min}). One can also observe the close resemblance of the spectra between $W + \geq 1$ jet and $Z + \geq 1$ jet events. The leading E_T spectra are generally harder for $W/Z + \geq 2$ jet than ≥ 1 jet events. This is because the leading jet needs to carry enough energy in order to radiate the second jet for $W/Z + \geq 2$ jet events.

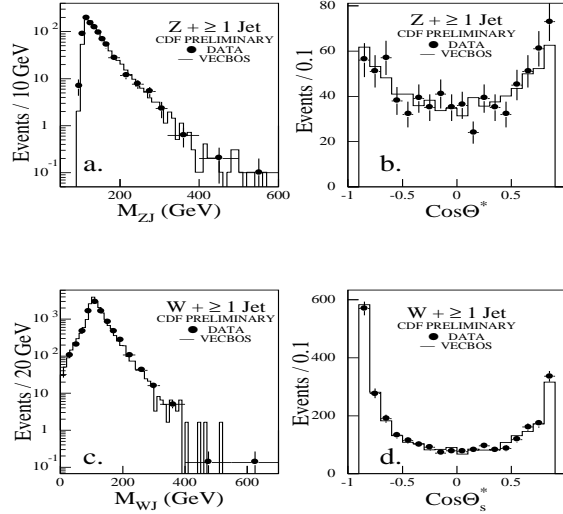


FIG. 2. (a)[c] Invariant mass distributions of $Z[W]$ and the leading E_T jet for $Z[W] + \geq 1$ jet events. (b)[d] Center of mass angular distributions of the leading jet for $Z[W] + \geq 1$ jet events. Solid circles represent the data and the histograms illustrate LO predictions.

B. Invariant mass of the $W/Z + N$ jet system and the angular distributions of the bosons

The invariant mass distributions of $W/Z + N$ jet final states can provide information on a new particle decaying to $W/Z + N$ jet final states. Figures 2(a) and (c) show the invariant mass distribution for Z and $W + \geq 1$ jet final states, respectively. Solid circles represent the data and the histograms indicate LO predictions. The data is well described by the predictions and no significant deviation from QCD expectation is observed within the given statistics.

The angular distribution of final state partons in the center of mass system depends on the spin of the mediator. The dijet final state at the Tevatron energy is dominated by gluon exchange. The gluons have spin 1 so that the angular distribution of the jets follows the Rutherford scattering pattern: $1/(1 - \cos\theta^*)^2$, where θ^* is the polar angle of the leading jet in the center of mass system. However, the $W/Z +$ jet final state is dominated by spin 1/2 quark exchange. Therefore the angular distributions of the W and Z bosons are expected to follow $1/(1 - \cos\theta^*)$. Figures 2(b) and (d) show the angular distributions of the bosons in the Z and $W + \geq 1$ jet events, respectively, along with the LO QCD predictions. One can observe that within the statistics the angular distributions are well described by the LO theoretical prediction.

C. Invariant mass distributions of the two jets and the spatial correlations between the two jets

The invariant mass distributions of the jets in QCD multijet final states can provide a signature of resonances. The invariant mass of the two jets in the $W/Z + \geq 2$ jet final states could also indicate a new resonance produced along with the bosons and decay to

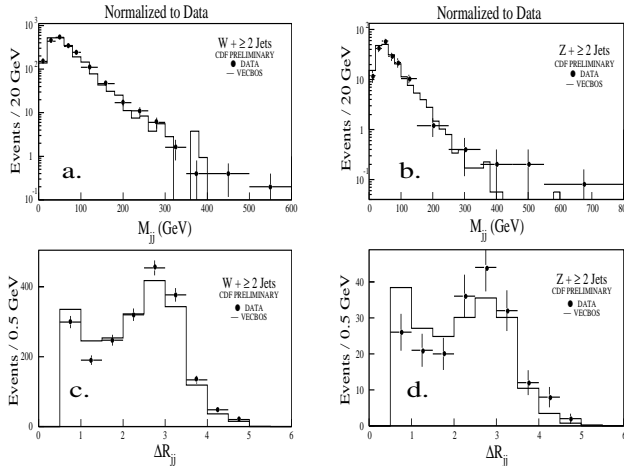


FIG. 3. (a)[b] Invariant mass distributions of the leading two jets in $W[Z] + \geq 2$ jet events. (c)[d] Spatial distance between the two leading jets in $W[Z] + \geq 2$ jet events. Solid circles represent the data and the histograms illustrate LO predictions.

two jets. Figures 3(a) and (b) show the invariant mass distributions of the two jets in the W and $Z + \geq 2$ jet final states, respectively. The solid circles represent the data and the histograms indicate LO predictions. The data distributions are well described by the theoretical predictions and no indication of resonances is observed.

Figures 3(c) and (d) show the distance between the two jets in $\eta - \phi$ space, $\Delta R_{jj} \equiv \sqrt{(\Delta\eta)^2 + (\Delta\phi)^2}$, for W and $Z + \geq 2$ jet final states in comparison with the LO predictions, respectively. While the two distributions show remarkable resemblance, there are systematic disagreements between the LO predictions and the data for both W and $Z + \geq 2$ jet events. In particular, statistically significant deviations can be observed at $\Delta R_{jj} \sim 0.5$ and ~ 3 .

III. W/Z+JET MULTIPLICITY DISTRIBUTIONS

An accurate measurement of jet multiplicity distributions associated with W and Z bosons is needed because these processes are one of the major background sources to $t\bar{t}$ production. However, since only tree level calculations exist for processes with jet multiplicities greater than one, the uncertainty in the normalization of the predictions increases with the increasing number of jets. The jet multiplicity distribution associated with the W boson has been measured by the CDF experiment using 4.2 pb^{-1} of data taken during the 1989 Tevatron collider run (4). With the larger $W/Z + N$ jet samples, it is possible to measure the cross sections more accurately.

Since the probability of radiating an extra parton depends on the strong coupling constant α_s , the jet multiplicity distributions are expected to be proportional to $\mathcal{O}(\alpha_s^{N_{jets}})$ (5). Thus, one expects to observe a power law behavior in the multiplicity distributions. Figures 4(a) and (b) show the jet multiplicity distributions associated with the W bosons decaying into $e + \nu$ and the Z bosons decaying into $e^+ + e^-$, respectively, from the CDF experiment. Solid circles indicate the data and the lines are straight lines drawn by hand to guide the eyes. One can observe the power law behavior of the distribution down to $W + \geq 6$ jet events in Fig 4(a). The same trend can be observed for Z bosons in Fig 4(b), as

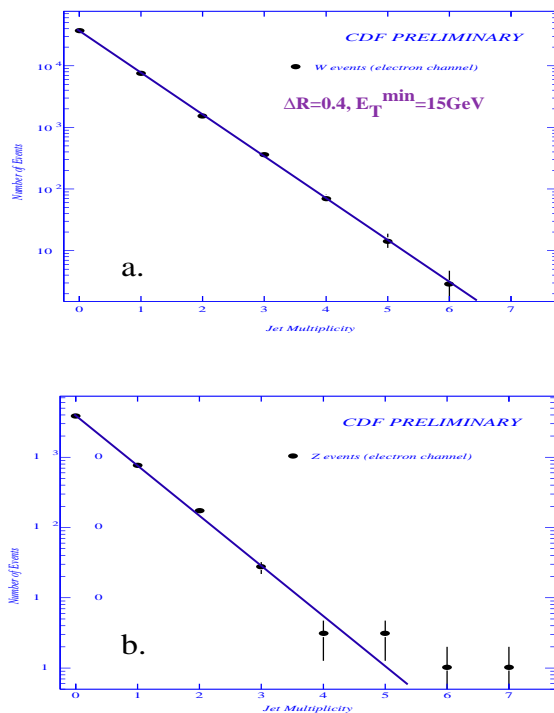


FIG. 4. Jet multiplicity distributions for W and Z bosons for (a) $W \rightarrow e + \nu$ decay and (b) $Z \rightarrow e^+ + e^-$ decay channel. The lines are not fits but hand drawn to guide the eyes. The jets in these distributions are defined with radius of 0.4 and $E_T^{\min} = 15$ GeV.

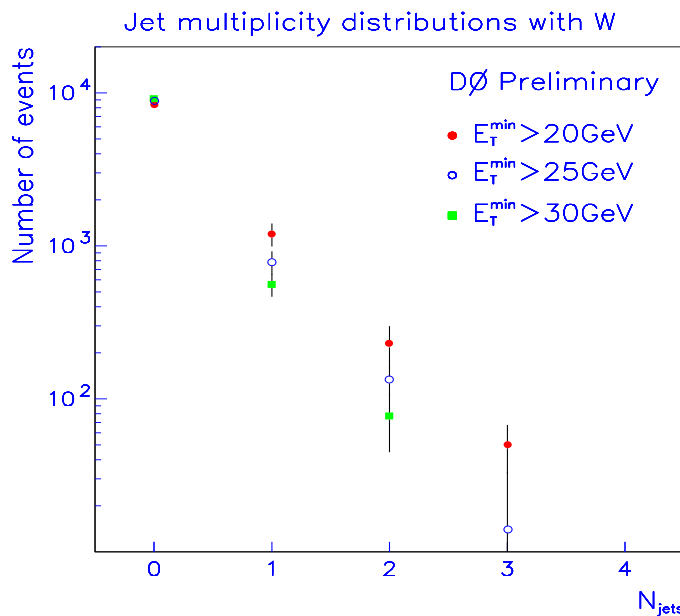


FIG. 5. Jet multiplicity distributions for $W \rightarrow e\nu$ decay channel for various E_T^{\min} cuts for jets. The cone radius is 0.7.

well. The jets in these distributions are defined with a fixed cone algorithm with radius $\Delta R = \sqrt{(\Delta\eta)^2 + (\Delta\phi)^2} = 0.4$ and jet minimum E_T cutoff, $E_T^{min} = 15$ GeV. Since the masses and couplings of W and Z bosons are not much different, one would expect to see that the production mechanisms do not differ greatly from each other. One can see that the shapes of the two distributions and the slopes of the two lines are very similar.

Figure 5 shows the jet multiplicity distributions associated with $W \rightarrow e + \nu$ candidates from the $D\phi$ experiment. Different symbols represent different jet definitions with varying E_T^{min} . The jet algorithm is a fixed cone algorithm with the cone radius $\Delta R = 0.7$. One can clearly observe the power law behavior of the multiplicity distributions for all E_T^{min} values. One can also see that the distributions get steeper as the E_T^{min} increases from 20 GeV to 30 GeV. This is because the probability of a radiated parton satisfying the jet definition decreases with increasing E_T^{min} .

IV. A STUDY OF THE STRONG COUPLING CONSTANT

In tree level calculations, the cross section of the $W + 1$ jet process is proportional to the strong coupling constant, α_s , whereas the cross section of the $W + 0$ jet process is independent of α_s . Therefore, the ratio of the $W + 1$ jet to $W + 0$ jet cross section is proportional to α_s (6,7). The $D\phi$ experiment used to exploit this property to determine the value of α_s at the mass of the W (M_W), using next-to-leading order (NLO) predictions (8).

Using 9770 $W \rightarrow e + \nu$ candidates collected during the 1992-93 Tevatron collider run, the $D\phi$ experiment measured the ratio of the $W + 1$ jet to the $W + 0$ jet cross sections, \mathcal{R}_{exp} , for various E_T^{min} values. The jets are defined with a fixed cone algorithm with $\Delta R = 0.7$. Figure 6 shows the measured ratio, \mathcal{R}_{exp} , as a function of E_T^{min} . Solid circles are the data, the solid lines represent NLO predictions for two different values of α_s , and the dashed lines indicate the same for LO predictions, using MRSD0 parton distribution functions (pdf) (10). As one expects, the ratio \mathcal{R}_{exp} decreases as E_T^{min} increases. This trend is well described by both LO and NLO predictions. It is also clear from the figure that the predicted ratio is sensitive to the variation of α_s . In these theoretical predictions, α_s was varied only in the hard partonic cross sections ($\hat{\sigma}$).

In NLO predictions, the cross sections of the $W + N$ jet processes can be parameterized as $\sigma(W + N \text{ jet}) = \alpha_s^N (a_N + \alpha_s b_N)$. The ratio of the $W + 1$ jet to the $W + 0$ jet cross sections can then be expressed as $\mathcal{R}_{pred} = \alpha_s (a_1 + \alpha_s b_1) / (a_0 + \alpha_s b_0)$. The coefficients are computed by the NLO theoretical predictions for a given pdf. By equating this expression with the experimentally measured ratio \mathcal{R}_{exp} and solving the equation for α_s , a value of α_s can be obtained.

The $D\phi$ experiment used the measured ratio $\mathcal{R}_{exp} = 0.065 \pm 0.003(stat.) \pm 0.007(syst.)$ for $\Delta R = 0.7$ and $E_T^{min} = 25$ GeV to extract the value of α_s . At present, the uncertainty in this measurement is dominated by the experimental systematics due to the jet energy scale. Figure 7 shows \mathcal{R}_{exp} as a horizontal line along with its total uncertainty indicated by the shaded area. The symbols in the figure correspond to the NLO predictions of the ratio \mathcal{R}_{pred} with α_s fixed at the value associated with each pdf, evaluated at the scale $Q^2 = M_W^2$. The two lines represent the variations of \mathcal{R}_{pred} for CTEQ3M (11) and MRS(D'_0) (12) pdf when the value of α_s is varied in the hard partonic cross section only. The intercepts of these lines with the measured value \mathcal{R}_{exp} give a measure of α_s for each pdf.

Table 1 lists the extracted values of α_s , as described above, compared to the value of α_s for the given pdf, α_s^{pdf} , evolved to the scale $Q^2 = M_W^2$ using the two loop expression of α_s . One can observe that the extracted values are larger than the input values of α_s^{pdf} by over one standard deviation. One should note here that these values should not be treated as a

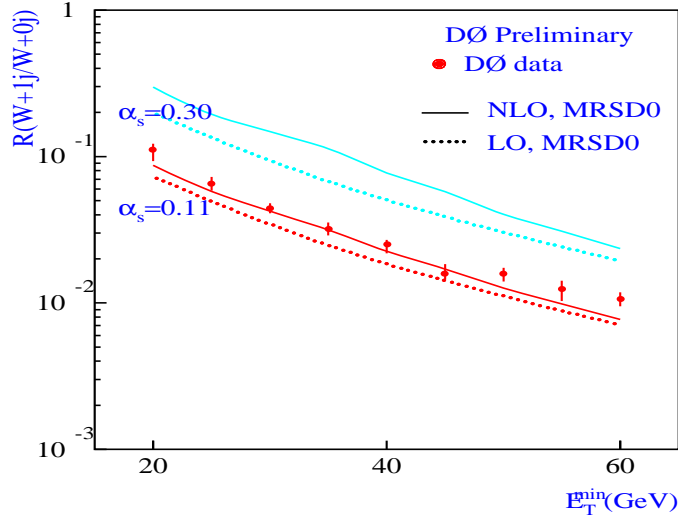


FIG. 6. \mathcal{R} vs E_T^{min} . Solid lines represent NLO predictions for two different values of α_s using MRSD0 parton distributions. The dashed lines represent LO predictions.

pdf	$\alpha_s(M_W) \pm \Delta\alpha_s$	$\alpha_s^{pdf}(M_W)$
CTEQ2M	0.134 ± 0.016	0.112
CTEQ2ML	0.139 ± 0.017	0.119
CTEQ2MF	0.132 ± 0.015	0.113
CTEQ2MS	0.131 ± 0.015	0.113
CTEQ3M	0.139 ± 0.017	0.114
MRS(D'_0)	0.129 ± 0.015	0.113
MRS(S'_0)	0.129 ± 0.015	0.113
MRS(D'_-)	0.136 ± 0.016	0.113
GRV92	0.129 ± 0.015	0.111

TABLE 1. The extracted values of α_s for given pdf in comparison with the input α_s values to pdf's.

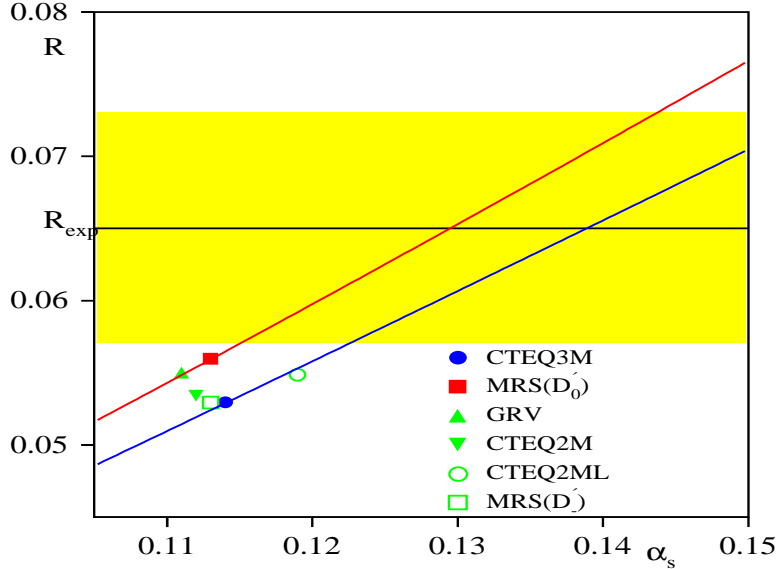


FIG. 7. Predicted ratio vs α_s for fixed α_s^{pdf} . The lines represent the variation of the ratio when α_s only in ME is varied.

universal value for α_s that can be directly compared to the results from LEP experiments, because this method of α_s determination fixes the α_s in the pdf's and varies α_s only in the hard partonic cross section.

The pdf's have an implicit dependence on the value of α_s through the evolution of the parton densities determined at the lower energy scale (Q_0^2) to the scale of interest ($Q^2 = M_W^2$ in this case). Therefore, in order to determine the strong coupling constant in a fully consistent manner, one needs to vary the value of α_s both in pdf and in $\hat{\sigma}$ simultaneously. This procedure requires a refitting of all the other parameters in pdf's for the given values of α_s or Λ_{QCD} (see for example Ref. (13–15)).

The UA2 experiment at $\sqrt{s} = 630$ GeV exercised the above procedure (6). They observed a slight correction to the slope compared to only varying α_s in $\hat{\sigma}$. The results of the same exercise carried out by the $D\bar{O}$ experiment $\sqrt{s} = 1800$ GeV are shown in Fig. 8 for three different families of pdf's. The symbols in Fig. 8 show the predictions for various families of pdf's fitted with several values of input α_s^{pdf} . The points representing the CTEQ3 family do not have error bars, because these points are statistically 100% correlated. The predicted behavior of \mathcal{R} shows that the sensitivity of the ratio to the value of α_s is greatly reduced. One possible cause of this decrease in the sensitivity could be the compensation of the increase in α_s in $\hat{\sigma}$ by the softening of the gluon distributions at our average parton momentum fraction, x , (~ 0.04) for $W + \text{jets}$ processes. This compensation occurs because the $W + 1$ jet cross section at the Tevatron energy ($\sqrt{s} = 1.8$ TeV) is dominated by the $q + g \rightarrow W + q$ process. In addition, the predictions using the latest families of pdf's (13–15) are consistently lower than the measured value of \mathcal{R}_{exp} by more than one standard deviation, no matter which family of pdf is used nor which value of input α_s is used. Although the level of disagreement is only about one standard deviation, it is interesting to see that all the families of pdf's show that they are consistent with each other and consistently lower than the data. If this

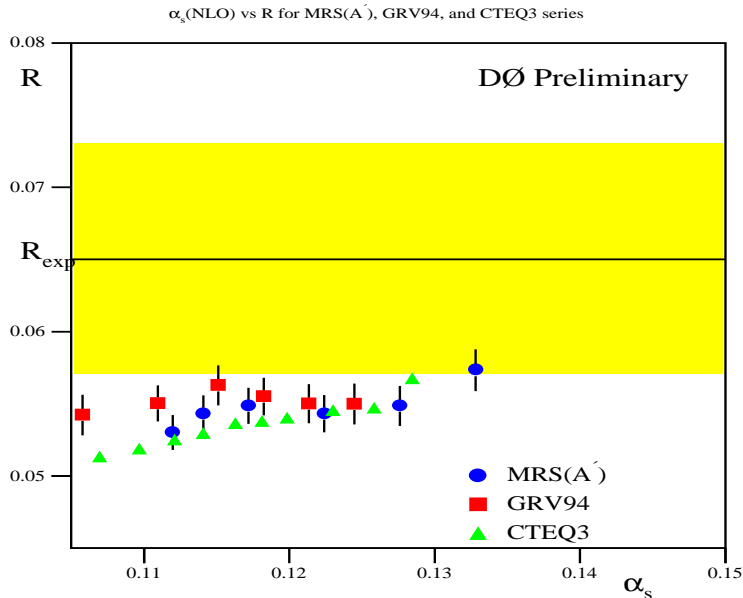


FIG. 8. Predicted ratio vs α_s for various input values of α_s^{pdf} for pdf evolution.

disagreement persists with more precise measurements, one would conclude that some new ingredient in the pdf's is needed to explain the W +jets measurements.

V. CONCLUSIONS

Using the large samples of W and Z bosons, the DØ and CDF experiments at Fermilab are intensively testing QCD predictions. Various kinematic quantities of the jets associated with the bosons show good agreement between data and theoretical predictions. Some statistically significant systematic disagreement start emerging in the two jet spatial distance in $W/Z + \geq 2$ jet events. The jet multiplicity distributions are measured and show the expected scaling behavior as a function of the multiplicity. The strong coupling constant has been extracted using the ratio of the $W + 1$ jet and $W + 0$ jet cross sections for various pdf's. The extracted values of α_s are consistently higher than those input to pdf's. A comprehensive study of α_s was performed using many modern pdf's fitted with various values of input α_s . The predicted ratio from several families of pdf's show that the sensitivity to the value of α_s is greatly reduced. The predictions are consistently lower than the experimental measurement by slightly over one standard deviation.

We are grateful to the DØ and CDF Collaborations for discussions of their data. We express our appreciation to the three pdf groups (MRS, CTEQ, and GRV) for providing us with the new fits of pdf's to carry out the study on the determination of α_s .

REFERENCES

1. Y. I. Azimov, Y. L. Dokshitzer, V. A. Khoze and S. I. Troyan, *Z. Phys.* **C27**, 65 (1985).
2. F.A.Berends, W.T.Giele, and H.Kuijf, *Nucl. Phys.* **B321**, 39 (1989).
3. J.Benlloch, CDF collaboration, Proceedings of DPF '92, 1091 (1993)
4. F.Abe *et al.*, CDF collaboration, *Phys. Rev. Lett.* **70**, 4042 (1993).
5. F.A.Berends, W.T.Giele, and H.Kuijf, *Nucl. Phys.* **B321**, 39 (1989);
F.A.Berends, W.T.Giele, H.Kuijf, and B. Tausk, *Nucl. Phys.* **B357**, 32 (1991).
6. J. Alitti *et al.*, *Phys. Lett.* **B263**, 563 (1991);
7. M. Lindgren *et al.*, *Phys. Rev.* **D45**, 3038 (1992).
8. W.T.Giele, E.W.N. Glover, and D.A.Kosower, *Nucl. Phys.* **B403**, 633 (1993).
9. Jaehoon Yu, Ph.D. Thesis, SUNY at Stony Brook, August, 1993 (Unpublished).
10. A.D.Martin, R.G.Roberts and W.J.Stirling, *Phys. Lett.* **B266**, 173 (1991).
11. H.L.Lai *et al.*, CTEQ collaboration, *Phys. Rev.* **D51**, 4762 (1995).
12. A.D.Martin, R.G.Roberts and W.J.Stirling, *Phys. Lett.* **B306**, 145 (1993).
13. A. Vogt, DESY preprint DESY-95-068 (1995).
14. A.D.Martin, R.G.Roberts and W.J.Stirling, Durham University preprint, DTP/95/48(1995).
15. H. Weerts, CTEQ collaboration, Private communication.